Low-dose JAK3 inhibition improves antitumor T-cell immunity and immunotherapy efficacy

Dammeijer, F.; Gulijk, M. van; Klaase, L.; Nimwegen, M. van; Bouzid, R.; Hoogenboom, R.; ... ; Aerts, J.G.

Low-Dose JAK3 Inhibition Improves Antitumor T-Cell Immunity and Immunotherapy Efficacy

Floris Dammeijer[1,2], Mandy van Gulijk[1,2], Larissa Klaase[1], Menno van Nimwegen[1], Rachid Bouzid[1], Robin Hoogenboom[1], Maria E. Joosse[2], Rudi W. Hendriks[1], Thorbald van Hall[3], and Joachim G. Aerts[1,2]

ABSTRACT

Terminal T-cell exhaustion poses a significant barrier to effective anticancer immunotherapy efficacy, with current drugs aimed at reversing exhaustion being limited. Recent investigations into the molecular drivers of T-cell exhaustion have led to the identification of chronic IL2 receptor (IL2R)–STAT5 pathway signaling in mediating T-cell exhaustion. We targeted the key downstream IL2R-intermediate JAK 3 using a clinically relevant highly specific JAK3-inhibitor (JAK3i; PF-06651600) that potently inhibited STAT5-phosphorylation *in vitro*. Whereas pulsed high-dose JAK3i administration inhibited antitumor T-cell effector function, low-dose chronic JAK3i significantly improved T-cell responses and decreased tumor load in mouse models of solid cancer. Low-dose JAK3i combined with cellular and peptide vaccine strategies further decreased tumor load compared with both monotherapies alone. Collectively, these results identify JAK3 as a novel and promising target for combination immunotherapy.

Introduction

Cancer immunotherapy induces durable antitumor immune and clinical responses but only in a minority of patients and tumor types for reasons still incompletely understood (1–3). T-cell exhaustion is a major mechanism underlying cancer immunotherapy resistance and current treatment strategies aimed at the prevention or reversal of exhaustion are lacking (4). T-cell exhaustion arises through chronic antigen stimulation of the T-cell receptor (TCR) in a suppressive tumor microenvironment (TME), decreasing T-cell functionality and persistence (5, 6). Attempts have been made to prevent T-cell exhaustion by inhibiting key downstream TCR-signaling pathways (e.g., MAPK/ERK, mTOR), yielding varying clinical and preclinical results (7–11). Possible redundancy between different signaling pathways and the existence of exhaustion mechanisms other than chronic TCR-activation could be involved in T-cell exhaustion and immunotherapy resistance.

Besides excessive TCR stimulation, continuous IL2 receptor (IL2R)–induced STAT5 phosphorylation in T cells has recently been linked to exhaustion in chronic viral infection and cancer, with $IL2^{hi}$ cancers exhibiting poor prognosis (12, 13). Despite that IL2 is required for initial T-cell expansion and survival, excess IL2 during T-cell priming skews toward a short-lived T-cell effector fate at the expense of memory precursor T cells (14, 15). Whether temporal downstream IL2R inhibition improves antitumor immunity is currently unknown. The IL2R may be a particularly attractive target as activation of the receptor culminates in MAPK-, mTOR- as well as STAT5-signaling, thereby allowing for concomitant targeting of multiple exhaustion-related pathways.

Binding of IL2 to the high-affinity IL2R consisting of α, β, and γ chains (CD25, CD122, and CD132, respectively) activates a downstream cascade initiated by JAK family members JAK1 and JAK3 that in turn phosphorylate STAT5 leading to dimerization and target gene transcription (16, 17). In contrast with JAK1 associating with various type I and II cytokine receptors, JAK3 is located downstream of the common-gamma chain cytokine receptor family, including IL2R, IL4R, IL7R, and IL15R. With the recent development of specific JAK inhibitors, interrogation of these downstream cytokine–receptors pathways has become feasible with minimal off-target activity (18). This allowed us to investigate JAK3 as novel immunotherapeutic target downstream of the IL2R using the highly specific JAK3-inhibitor (JAK3i) PF-06651600 (further referred to as PF-06) that was initially developed for treatment of autoimmune disease (19, 20). In this report, we demonstrate that this JAK3i effectively inhibits IL2-mediated STAT5 phosporylation in T cells and when administered at high-dose diminishes antitumor T-cell immunity. In contrast, at low-dose, PF-06 improves T-cell responses and decreases tumor load in solid tumor mouse models. Moreover, JAK3i potentiated cellular- and peptide-vaccine immunotherapies, improving therapeutic efficacy and reducing the exhausted T-cell phenotype. These important potential improvements of current immunotherapy warrant further investigation into the clinical use of low-dose JAK3i in patients with solid tumor.

Materials and Methods

Phosphoflow analysis

Wild-type C57BL/6 mice were euthanized by cervical dislocation and the spleens were isolated and mashed over a 100-μm filter establishing a cell suspension in RPMI-1640 containing 2% FCS. A total of 2×10^6 splenocytes were incubated for 3 hours at 37°C with vehicle (same amount of DMSO as highest concentration of inhibitor as negative control) or acalabrutinib (10, 1, and 0.1 μmol/L in DMSO) or Ibrutinib (10, 1, and 0.1 μmol/L in DMSO) or PF-06651600 (10, 1, and 0.1 μmol/L in deionized water (MilliQ), all obtained

[1]Department of Pulmonary Medicine, Erasmus MC, University Medical Center Rotterdam, the Netherlands. [2]Erasmus MC Cancer Institute, Erasmus MC, University Medical Center Rotterdam, the Netherlands. [3]Department of Medical Oncology, Oncode Institute, Leiden University Medical Center, the Netherlands.

Corresponding Authors: Floris Dammeijer, Pulmonary Medicine, Erasmus MC Rotterdam, PO Box 2040, Rotterdam, 3000 CA, the Netherlands. E-mail: f.dammeijer@erasmusmc.nl; and Joachim G. Aerts, j.aerts@erasmusmc.nl

Mol Cancer Ther 2022;21:1393–405

doi: 10.1158/1535-7163.MCT-21-0943

from Sigma-Aldrich). The cells were stimulated with anti-CD3/CD28 biotin in case of the stimulated samples or RPMI-1640 2% FCS for unstimulated samples. Afterwards, the cells were washed with RPMI-1640 2% FCS and stained with streptavidin PerCP Cy5.5 to establish receptor cross-linking. After washing, the samples were stimulated at 37°C for 1 minute for $pZAP70_{Y319}$ (pZAP70) and $pSLP76_{Y128}$ (pSLP76), 5 minutes for $pITK_{Y180}$ ($pITK_{180}$) 120 minutes for IkB and $pS6_{S240/244}$ (pS6). Ten minutes before the end of the stimulation a live/death marker was added. At the end of the stimulation, Fix/Perm was added and incubated at 37°C for 10 minutes followed by transfer on ice and wash with permeabilization buffer. After permeabilization, the samples were stained for 30 minutes with extracellular surface markers using a mAb-staining mix, including Fc-receptor–blocking antibodies (aCD16/32; Bioceros). After wash, the samples were stained for one of each of the following phosphoflow targets; pZAP70, pSLP76, pITK180, and pS6. In case of the unlabeled anti-pS6 antibody, a third staining step containing a PE-labeled anti-Rabbit antibody was necessary. For pIkB, a different staining protocol was used by which cells were fixed with paraformaldehyde incubated for 10 minutes at room temperature followed by permeabilization using 0.5% saponin in FACS. Cells were then stained with surface markers and anti-pIkB followed by acquisition for flow cytometry.

IL2 stimulation and pSTAT5 phosphoflow

A total of 24×10^6 splenocytes were divided over 12 wells of a 24-well plate and aCD3/CD28 Dynabeads (Thermo Fisher Scientific) were added in a 1:1 ratio for 72 hours in TCM to induce IL2R expression as assessed by upregulation of CD25. Dynabeads were extracted by magnet retrieval and 2×10^6 cells were incubated for 3 hours at 37°C with vehicle (same amount of DMSO as highest concentration of inhibitor as negative control) or Acalabrutinib (10, 1. and 0.1 μmol/L in DMSO) or Ibrutinib (10, 1, and 0.1 μmol/L in DMSO) or PF-06651600 (10, 1, and 0.1 μmol/L in deionized water). After 3 hours, a 500,000/50 μL cell suspension was activated for 15 minutes with 10 ng/mL IL2 (R&D Systems) at 37°C. Ten minutes before the re-stimulation end time, a live/death marker was added (eBioscience) followed by cell fixation using BD Cytofix and incubated for 10 minutes at 37°C. After the cells were fixed, the cells were washed with MACS buffer (PBS containing 5 mmol/L EDTA and 1% BSA) and permeabilized with 150 μL permbuffer III (BD Biosciences) and the cells were incubated for 30 minutes at −20°C. After 30 minutes the cells were washed with MACS buffer and stained with surface markers containing CD25, CD8, CD4, PD-1, CD44, B220, and CD3 and Fc-block for 30 minutes at 4°C followed by wash with MACS buffer and pSTAT5 staining for 30 minutes at room temperature.

Bone marrow–derived macrophage cultures

Bone marrow cells were isolated from the femurs and tibias of naïve CBA/J (Janvier), or C56BL/6 mice (Envigo, Zeist) mice under sterile conditions. In short, all muscle tissues are removed with gauze from the bones and placed in a 60-mm dish with 70% alcohol for 1 minute, washed twice with PBS, and transferred into a fresh dish with RPMI-1640. Bones were crushed using a pestle and mortar and subsequently passed through nylon mesh to remove small pieces of bone and debris followed by erythrocyte lysis using ammonium chloride. Bone marrow cells were resuspended in RPMI supplemented with 10% FCS, 2.5-mL gentamicin (10 mg/mL; Gibco), 50 μmol/L β-mercaptoethanol (Sigma-Aldrich) and 10 ng/mL M-CSF (R&D Systems) to establish macrophage-TCM. 2×10^5 cells were plated per well in a 24-well Nunc plate with Upcell surface coating, allowing for harvest of cells at low temperatures following a 7-day culture period. Fresh TCM was added on day 3 of culture, and polarizing cytokines with or without a range–drug concentrations on day 6 for the final 24-hour remainder of the culture period. M1 macrophages were generated by adding LPS (50 ng/mL) and IFNγ (50 ng/mL), or IL4 (10 ng/mL) with or without IL10 (10 ng/mL) or IL13 (10 ng/mL) in case of M2 macrophages. Besides the inhibition of JAK3 using the specific JAK3-inhibitor (PF06651600, Sigma-Aldrich), cells were alternatively treated with trimeric CD40 L (Immunex, 1 μg/mL), with a JAK1/JAK3 dual inhibitor (Tofacitinib, Sigma-Aldrich) or associated diluents as negative controls. At the end of the culture, the plates were put on ice and cell suspensions were harvested and prepared for flow-cytometric analysis.

Monocyte-derived macrophage cultures

Venous blood from adult healthy individuals was collected in EDTA tubes and peripheral blood mononuclear cells (PBMC) were isolated using a Ficoll-Hypaque gradient according to standard protocol (Axis-Shield Diagnostics). Written informed consent was obtained from the donors and studies were conducted in agreement with the Declaration of Helsinki, according to the ICH Harmonized Tripartite Guideline on Good Clinical Practice and in accordance with recognized ethical guidelines approved by our local institutional review board. Monocytes were extracted with magnetic-activated cell sorting (MACS) using anti-CD14 antibody coated microbeads (Milteny Biotec) according to the manufacturer's protocol. Following the MACS-procedure, cells were stained for flow cytometry to guarantee sufficient purity (>98%). Monocytes were then suspended in TCM consisting of RPMI-1640 + Glutamax, 10% normal healthy AB serum and human macrophage colony-stimulating factor (20 ng/mL; R&D Systems). Cells were cultured similarly to murine macrophages, with the exception of being an 8-day culture with macrophage polarization occurring in the final 48 hours of culture. Polarization to the M1 or M2 phenotype occurred in the presence of LPS (100 ng/mL; Sigma-Aldrich) and IFNγ (20 ng/mL; R&D Systems) for M1 or IL4 (20 ng/mL, R&D Systems) with or without IL13 (20 ng/mL; R&D Systems) for M2 for 2 days.

Bone marrow–derived dendritic cell–OT-I and tumor-cell co-culture

Bone marrow–derived dendritic cells (BMDC) were cultured from $n = 3$ wild-type C57BL/6 donor mice (female, 8 weeks) similarly to bone marrow–derived macrophages (BMDM) but GM-CSF instead of M-CSF was used as a growth factor for 9 days of culture in normal tissue-culture coated 6-well plates (Sarstedt), followed by 24 hours of simulation with OVA-protein (150 μg/mL) and CpG in the presence of JAK3i (PF06651600, Sigma-Aldrich) as reported previously and analyzed using flow cytometry (21). Next, OT-I cells were sorted from spleens and lymph nodes of female OT-I mice bred in house using a $CD3^+$ negative selection kit (EasySep; StemCell) followed by cell labeling using CellTrace Far Red proliferation dye (Invitrogen) according to the manufacturer's protocols. Labeling efficacy and OT-I purity were checked using flow cytometry before co-culture. A total of 5.0×10^3 non-JAK3i pre-treated SIINFEKL-peptide (500 ng/mL)–loaded BMDCs were co-cultured with 2.5×10^4 naïve labeled and purified OT-I T cells in 96-well flat-bottom plates using T-cell medium (IMDM supplemented with 10% FBS, β-mercapto-ethanol and gentamicin) and JAK3i in a 1:5 (DC–T-cell) ratio for 72 hours and harvested or for subsequent co-culture with AE17-OVA tumor cells for 24 hours (ratio: 1:1) followed by for flow-cytometry analysis. T-cell mono-cultures.

Human T-cell cultures

PBMCs from healthy donors were labeled with CellTrace Violet (Thermo Fisher Scientific) and were stimulated with anti-CD3/CD28 Dynabeads at 0.5 bead per mononuclear cell with or without recombinant human IL2 (1, 10 or 100 IU/mL, R&D Systems) for the indicated time-points. In some conditions, Tofacitinib (200 or 1,000 μmol/L) or PF-06651600 (200 or 1,000 μmol/L) was added to the culture. Cells were cultured in IMDM (Thermo Fisher Scientific) supplemented with heat-inactivated FCS, Glutamax (Thermo Fisher Scientific), 2-mercaptoethanol, penicillin, and streptomycin. Cytokine concentrations in cell supernatants were analyzed using an ELISA set for IFNγ (eBioscience) according to the manufacturer's instructions. In case of murine T-cell cultures, proliferation-dye pre-stained wild-type C57BL/6 T cells were stimulated with anti-CD3/CD28 Dynabeads at 1:1 ratio with various concentrations of PF06651600 (negative control = H_2O) or tofacitinib (negative control = DMSO) and assessed for proliferation, activation (CD69 and CD25) and cytokine (TNF-alpha and IFN-gamma) production 24 hours later using (intracellular) flow cytometry.

In vivo murine tumor models and experiments

Female 8–10-week-old C57BL/6 mice (Envigo, Zeist) and CBA/J mice (Janvier) were housed under specific pathogen-free conditions at the animal care facility of the Erasmus MC, Rotterdam. Experiments were approved by the local and central Ethical Committee for Animal Welfare and complied to the Guidelines for the Welfare of Animals in Experimental Neoplasia by the United Kingdom Coordinating Committee on Cancer Research (UKCCCR) and by the Code of Practice of the Dutch Veterinarian Inspection. The AE17 cell and AC29 mesothelioma cell lines were kindly provided by Bruce W.S. Robinson of the Queen Elizabeth II Medical Center (Nedlands, Australia) who previously authenticated these cells as being mesothelioma cells. At every 8–10 passages, cell lines were tested for *Mycoplasma* contamination by PCR and remained negative. Tumor cells were cultured in RPMI-1640 medium containing 25 mmol/L HEPES, Glutamax, 50 g/mL gentamicin, and 5% (v/v) FBS (all obtained from Gibco) in a humidified atmosphere and at 5% CO_2, in air. For culture, either culture flasks or CellSTACKs (Corning Life Sciences) were used to reach appropriate tumor cell frequencies for injection. AE17 and AC29 cells were passaged once or twice a week to a new flask by treatment with 0.05% trypsin, 0.53 mmol/L EDTA in PBS (all Gibco). At the start of the experiment, CBA/J or C57BL/6 mice were intraperitoneally or subcutaneously injected with either 10^7 AC29 cells or 0.5×10^6 AE17 cells, respectively, dissolved in PBS, or with PBS as control. Mice were scored using the body condition score, killed when body condition score was below 2 and scored as a death in the survival analysis. For DC-therapy experiments, BMDCs were generated from wild-type CBA/J mice and loaded with AC29 tumor cell lysate *in vitro* as described previously (21). On day 10 following intraperitoneal tumor inoculation, $2–3\times10^6$ DCs pre-loaded with AC29 tumor lysate and stimulated with CpG were injected intraperitoneally (21). For SLP (synthetic long peptide)-vaccination studies in the TC-1 tumor model, TC-1 cells were cultured in 500-mL IMDM medium, 8% FBS (40 mL) and pen/strep plus L-glutamin and following cell harvest were injected in the flank of wild-type C57BL/6 mice. When tumors were established on day 8, mice received subcutaneous PBS or the SLP HPV16 E743–77 (GQAEPDRAHYNIVTFCCKCDSTLRLCVQSTHVDIR) emulsified at a 1:1 ratio with Incomplete Freunds Adjuvant (IFA; Difco) in the contralateral flank. In case of subcutaneous tumor models, tumors were measured twice weekly using an electronic micro-caliper and mice were euthanized when tumors grew beyond 100 mm^2 or became ulcerated.

In vivo treatment with PF-06651600

Mice were treated with a range of PF-06651600 concentrations dissolved in pre-warmed deionized water (Milli-Q) with all tested concentrations ranging within the solubility spectrum (5 mg/mL). Mice were treated with the JAK3-inhibitor or the diluent (deionized water) via oral gavage, twice daily with intervals of 12 hours, as reported by the manufacturer for a maximum of 14 days. Alternatively, PF-06651600 was administered in drinking water *ad libitum*, assuming that 8-week-old female mice with an average weight of 20 g drink approximately 5 mL of water per 24 hours (meaning that for the 5 mg/kg dose in drinking water, 10 mg of PF-06651600 was dissolved in 1 L of deionized water, amounting to an approximately 25 μmol/L). Drinking water was refreshed every week and bottles were covered with aluminum foil.

Preparation of single-cell suspensions from tissues

Single-cell suspensions were generated from the spleens, blood, and tumors of mice from each group. All tissues were either weighed in a microbalance in case of tumors and spleens, or volume determined for blood. Briefly, spleens were aseptically removed and mechanically dispersed over a 100-μm nylon mesh cell strainer (BD Biosciences) followed by erythrocyte lysis using osmotic lysis buffer (8.3% NH4Cl, 1% $KHCO_3$, and 0.04% Na2EDTA in deionized water). Blood was collected in EDTA tubes (Microvette CB300, Sarstedt) and subsequently lysed. Tumors were collected, and dissociated using a validated tumor dissociation system (Miltenyi Biotec). Cells suspensions were filtered through a 100-μm nylon mesh cell strainer (BD Biosciences) and counted in trypane blue with a hemocytometer using the Burker–Turk method.

Immunomonitoring using flow cytometry

For measurements of cytokine production in lymphoid cells by flow cytometry, cells were restimulated for 4 hours at 37°C using PMA and ionomycin supplemented with GolgiStop (BD Biosciences). For assessing cytokine production by myeloid cells, cells were subjected to 4 hours incubation with Golgistop. For cell surface marker staining, cells were washed with FACS-wash (0.05% NaN3, 2% BSA in PBS) and Fc II/III receptor blocking was performed using anti-mouse 2.4G2 antibody (1 : 300; kindly provided by L. Boon, Bioceros, Utrecht, the Netherlands). After the blocking procedure, antibodies (all derived from BD Biosciences, BioLegend or Thermo Fisher Scientific, titrated to optimal dilutions and used according to the manufacturer's protocol) for cell surface staining were added into each sample and placed on ice for 30 minutes. Cells were washed in FACS-wash followed by a PBS wash, and then stained for viability using fixable LIVE/DEAD aqua cell stain (Thermo Fisher Scientific, 1:200). After two additional washes with FACS-wash, cells were either measured or in case of intracellular staining; fixed, permeabilized, and stained using Fix/Perm buffer (in case of nuclear protein staining, eBioscience) or 4% PFA and 0.5% saponin (in case of cytokine/granzymeB stainings, Sigma-Aldrich). Antibodies were stained for 30 minutes in case of the PFA/Saponin protocol and 60 minutes for the intranuclear staining protocol, on ice in the dark. A fixed number of counting beads (Polysciences Inc.) was added before data acquisition to determine the absolute amount of cells. Data were acquired using an LSR II flow cytometer (BD Biosciences) equipped with three lasers and FACSDiva software (BD Biosciences) and analyzed by FlowJo (Tree Star Inc.) software V10.1.

Tumor cell apoptosis assay

A total of 0.2×10^6 cells from various murine and human cancer–derived cell lines were cultured in aforementioned appropriate culture conditions in 6-wells plates for 48 hours in the presence of absence of different JAK3i (PF-06651600) concentrations. Following culture, cells were harvested and stained for cell death and apoptosis using the 7-AAD/Annexin V staining kit, according to the manufacturer's protocol (BioLegend).

Statistical analysis

Data are expressed as means with SEM. Comparisons between groups were made using one-way ANOVA tests where experimental treatment groups were compared with vehicle, or the Wilcoxon signed rank test in case of paired samples. When correlations were depicted, Spearman's rank correlation test was performed to test for statistical significance. A two-tailed value of $P < 0.05$ was considered statistically significant. Survival data were plotted as Kaplan–Meier survival curves, using the log-rank test to determine statistical significance. Data were analyzed using GraphPad Prism software (GraphPad, V5.01)

Results

PF-06 is a potent inhibitor of IL2-mediated STAT5-phosphorylation in T cells

Chronic phosphorylation of STAT5 by JAK1/3 in T cells has been recently found to underlie ineffective antitumor immunity providing a rational for JAK3i in solid tumors (12). Because JAKs are involved in many pro- and antitumor cytokine receptor pathways, off-target specificity of early-generation JAK3i could potentially antagonize beneficial outcomes of JAK3-specific inhibition at the expense of increased toxicity (18). To evaluate whether the novel compound PF-06 specifically inhibits STAT5-phosphorylation and to which degree, wild-type naive and pre-activated $CD25^+$ murine T cells were simulated *in vitro* using anti-CD3/CD28 or IL2, respectively, and analyzed using Phospho flow (22). The broad kinase inhibitor Ibrutinib was applied as a positive control because kinomescan data identified multiple kinases, including JAK3 as targets (23). The selective BTK-inhibitor Acalabrutinib was used as a negative control in our studies as BTK is not expressed by T cells (23, 24). Only PF-06 specifically inhibited IL2-mediated pSTAT5 in both $CD8^+$ and $CD4^+$ T cells (**Fig. 1**) while leaving other quintessential T-cell signaling pathways (e.g., downstream TCR and NF-κB unaltered (**Fig. 2**; Supplementary Fig. S1). As CD25 expression among $CD25^+$ T cells varied, we compared pSTAT5 levels at baseline and in response to JAK3i in CD25-high, intermediate- and low-expressing T cells. CD25-high–expressing cells displayed increased STAT5-phosphorylation at baseline but also in response to low-dose JAK3i *in vitro* suggesting increased sensitivity to IL2 in CD25-high–expressing cells (Supplementary Fig. S2A). Regulatory T cells (Treg) constitutively express CD25 as a means to scavenge IL2 thereby inhibiting effector T-cell proliferation (25). To investigate how Tregs respond to IL2 and JAK3i, we assessed pSTAT5-phosphorylation status in $CD44^+$ $CD25^{hi}$ $CD4^+$

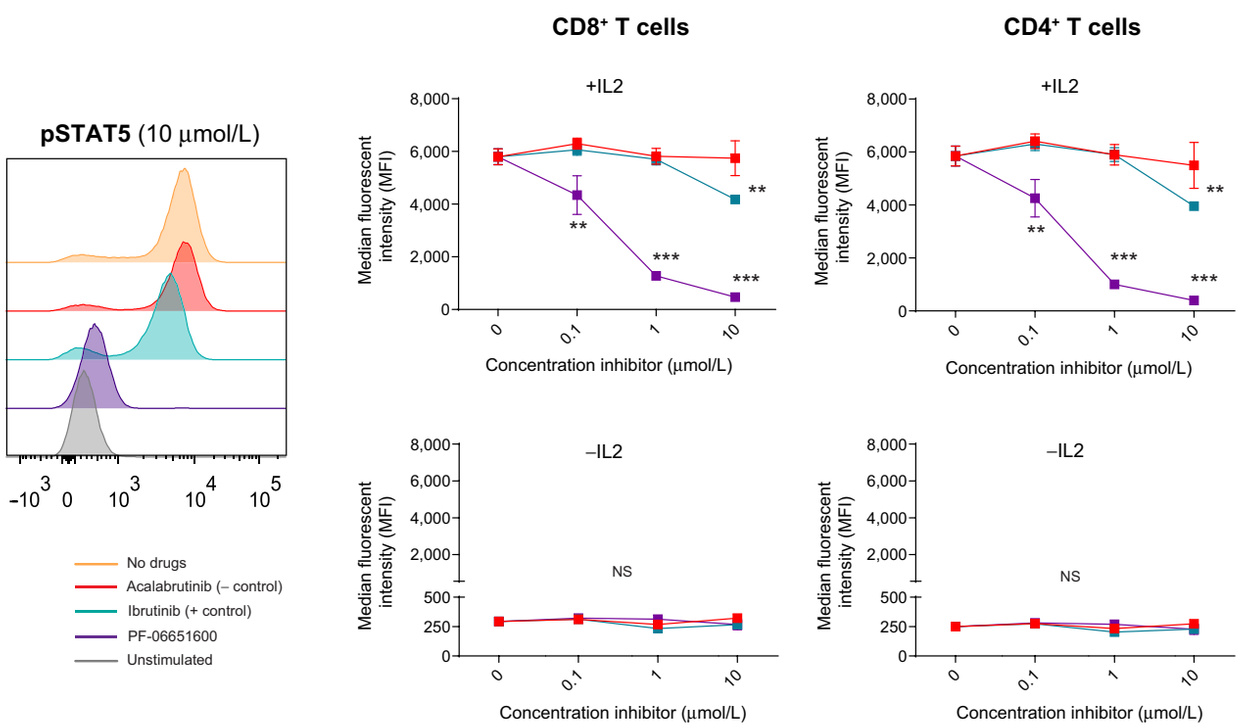

Figure 1.

The JAK3-inhibitor PF-06651600 potently inhibits STAT5-phosphorylation in response to IL2 in T cells. Preactivated IL2Rα (CD25)–expressing murine T cells were stimulated with IL2 after preincubation alone (orange), with the specific JAK3i; PF-06651600 (purple), aspecific JAK3i; Ibrutinib (turquoise) or negative control; acalabrutinib (red) using Phosphoflow. Histograms are shown displaying the effects of the different inhibitors on pSTAT5-expression at 10 µmol/L (left, $CD8^+$) and quantified expression of pSTAT5 in $CD8^+$ and $CD4^+$ T cells stimulated or unstimulated with IL2 (right). MFI, median fluorescence intensity; **, $P < 0.01$; ***, $P < 0.001$. Means and SEM are shown, $n = 5$/condition.

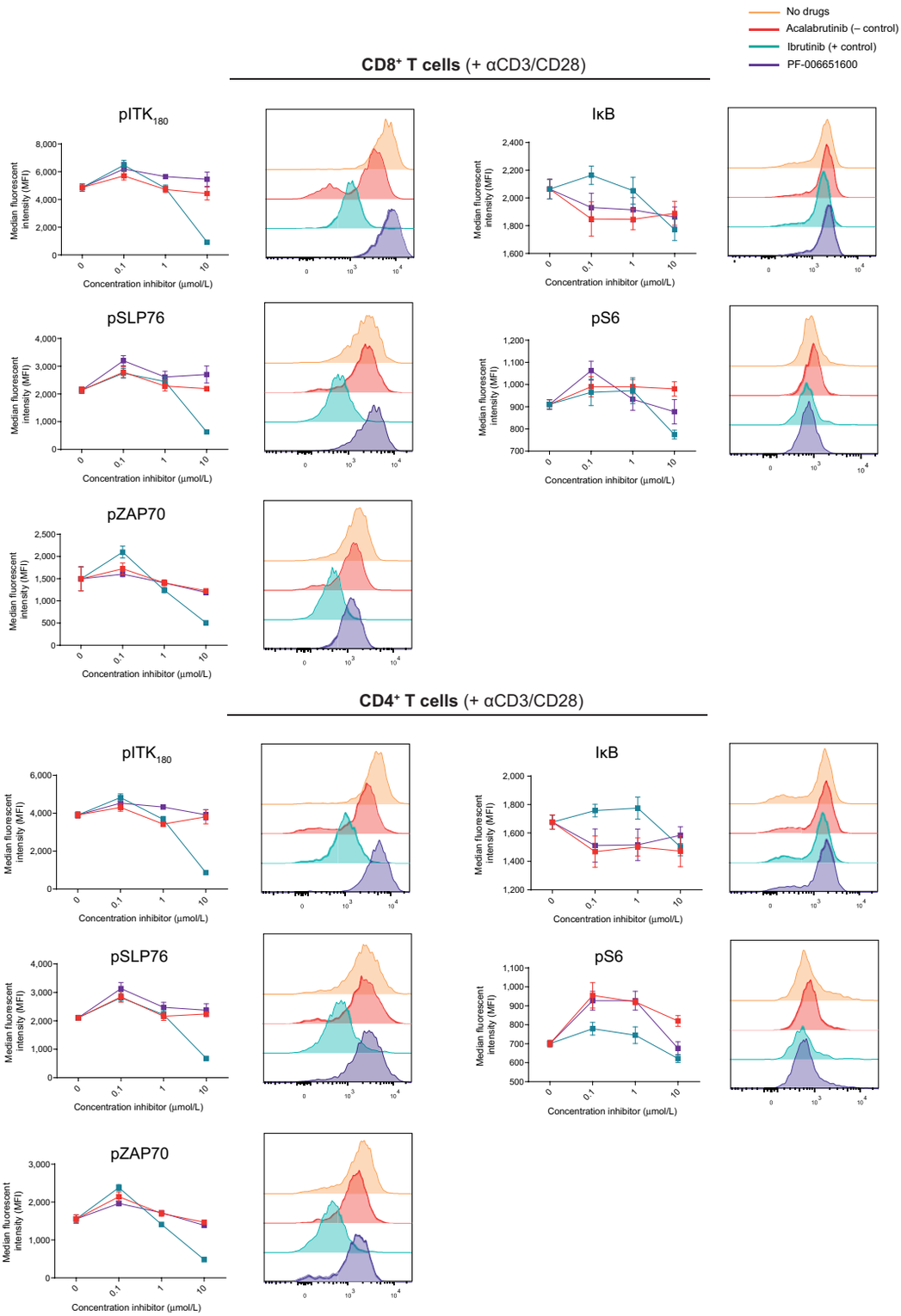

Figure 2.

PF-06651600 does not inhibit other T-cell signaling pathways. To determine off-target efficacy of PF-06 on other crucial T-cell signaling pathways, we assessed phosphorylation of proteins downstream of the T-cell receptor (TCR; pZAP70, pSLP76, and pITK180), PI3K-Akt (pS6), NF-kB (IKB), or MAPK-ERK (pERK) pathways following anti-CD3/CD28 stimulation with or without inhibitors using Phosphoflow. Results for both $CD8^+$ (top) and $CD4^+$ T cells (bottom) are shown as histograms (10 μmol/L drug concentration) and line graphs. MFI, median fluorescence intensity; means and SEM are shown, $n = 5$/condition.

T cells, a population enriched for Tregs in the naïve spleen (Supplementary Fig. S2B). As expected, pSTAT5-expression was nearly twice as high in Tregs compared with non-Tregs, with pSTAT5 being completely inhibited only at higher micromolar levels of PF-06 *in vitro* (Supplementary Fig. S2B). We concluded that the specific JAK3i PF-06 efficiently prevented STAT5 phosphorylation in mouse T cells in a low micromolar range.

PF-06 inhibits T-cell proliferation and effector function at high concentrations *in vitro*

To investigate how decreased IL2-mediated STAT5-phosphorylation translates to T-cell proliferation over time, we stimulated dye-labeled T cells *in vitro* using anti-CD3/CD28 Dynabeads alone or in the context of JAK3i. Head-to-head comparison between PF-06 and the less specific JAK1/3i Tofacitinib showed both drugs to inhibit T-cell proliferation, activation and effector cytokine production but only at high (>1.0 μmol/L) drug concentrations in mouse (Supplementary Fig. S3) and human (Supplementary Fig. S4A–S4C) T cells. Interestingly, whereas tofacitinib more potently inhibited T-cell proliferation and cytokine expression in humans compared with PF-06, the opposite was true for mice (Supplementary Figs. S3 and S4). In contrast with Tofacitinib, however, PF-06 only modestly inhibited cellular activation and IFNγ production in healthy-control–derived T cells at the micromolar range (Supplementary Fig. S4C). These findings show PF-06 to be a potent inhibitor of IL2-mediated pSTAT5 in T cells, with T-cell functions being inhibited only at higher drug concentrations providing a window for STAT5 modulation.

JAK3i decreases tumor progression depending on the dose and mode of administration

To assess the effects of PF-06 *in vivo* and its antitumor efficacy, we treated AE17 and AC29 immune competent mesothelioma tumor-bearing mice with PF-06 administered by oral gavage twice-daily as described by others (19). Using this treatment scheme, tumor progression was unaltered in these tumor models compared with vehicle treatment (**Fig. 3A**). The lack of response was accompanied by a reduction in T-cell proliferation monitored in peripheral blood (PB), and decreased activation, proliferation and effector function at the tumor site (**Fig. 3B**), indicative of suppressed antitumor immunity. We postulated that peak PF-06 concentrations following oral administration would approach immune suppressive drug concentrations reminiscent of aforementioned *in vitro* studies (Supplementary Fig. S3), and that low-grade and stable dosing of JAK3i in drinking water would ameliorate this issue. Therefore, we repeated the *in vivo* experiment dissolving PF-06 in drinking water aiming for tonic inhibition of the IL2R/JAK3/STAT5-axis throughout the antitumor immune response. In contrast with oral gavage, continuous low-dose JAK3i-suppressed tumor growth with approximately 25 μmol/L being established as the optimal dose (**Fig. 4A**). Changes in tumor burden were paralleled by increased T-cell frequencies and a more activated and proliferative T-cell compartment as evidenced by increased Ki-67 and PD-1 expression (**Fig. 4B**; Supplementary Fig. S5). B and NK cells on the other hand were not, or only marginally affected by JAK3i treatment (Supplementary Fig. S5). These data show that JAK3i, if provided as a steady continuous administration, impedes tumor progression coinciding with increased T-cell activation. In contrast with *in vitro*, macrophage polarization is not altered by JAK3i *in vivo*.

As JAK3 associates with cytokine receptors on other immune cells, treatment efficacy could potentially be explained by inhibition of alternative pathways, including IL4/IL4R signaling. Indeed, BMDMs stimulated *in vitro* with IL4 upregulated the M2 markers CD206, arginase and PD-L1 that could be antagonized by JAK3i (Supplementary Fig. S6A). This effect could not be rescued by addition of excess IL13, another M2-inducing cytokine sharing the IL4R-alpha subunit, or IL10 (Supplementary Fig. S6B (26, 27). In contrast with the JAK1/3i Tofacitinib, PF-06 did not alter pro-inflammatory (M1) macrophage differentiation as evaluated by iNOS and MHCII expression (Supplementary Fig. S6C). Similar findings were obtained using human monocyte–derived macrophages (Supplementary Fig. S7). Tumor-associated macrophage and conventional DC frequency and phenotype, however, were largely unaltered by JAK3i in all our investigated models, indicating that IL4 plays an inferior or redundant role in *in vivo* myeloid cell polarization (Supplementary Fig. S6D and S6E). On the same line, JAK3i did not directly affect solid tumor-cell apoptosis *in vitro* (Supplementary Fig. S8A) or *in vivo* (Supplementary Fig. S8B), except in case of the JAK3-mutated T-cell lymphoma cell line Hu-78 (Supplementary Fig. S8A). We concluded that T cells are the most likely direct targets of JAK3i.

Although JAK3i as monotherapy is capable of inhibiting tumor progression, combining JAK3i with existing immunotherapies could further enhance efficacy of both modalities. Cellular and peptide cancer vaccines are safe and efficacious in inducing antitumor T-cell responses in solid advanced cancer, but durable responses are obtained in a small minority of patients possibly due to the eventual exhaustion of vaccine-elicited T-cell responses (21, 28–32). To improve vaccine-induced T cells and treatment efficacy, we treated AC29-bearing mice, at late-stage, with tumor-lysate–loaded BMDCs in the presence or absence of JAK3i (**Fig. 5A**). We found JAK3i–DC combination immunotherapy to effectively reduce tumor load compared with both monotherapies alone (**Fig. 5B**). Similarly, we combined JAK3i with an SLP vaccine in the aggressive TC-1 solid tumor model showing similar combination immunotherapy efficacy, improving response rates, and reducing heterogeneity in tumor responses observed (**Fig. 5C–E**). Further investigations into the immunological mechanisms underlying combination immunotherapy efficacy in end-stage tumors revealed JAK3i to spare $CD8^+$ T-cell proliferation and boost TIL activation as indicated by increased CD25 and PD-1 but not CTLA-4 expression (**Fig. 6A**). In line with an activated rather than exhausted TIL phenotype was a specific increase in single PD-1–expressing TILs ($PD\text{-}1^+$ $CTLA4^-$) rather than inhibitory receptor double-positive TILs known to be exhausted (33, 34). Recently, the surface molecule CD39 was reported to mark activated, (pre-)exhausted and tumor-specific $CD8^+$ and $CD4^+$ T cells in the TME and this marker was significantly upregulated in combination immunotherapy-treated TILs compared with TILs derived from untreated- or JAK3i-only treated mice (35, 36). Besides surface molecules, combination immunotherapy-treated TILs displayed highest levels of IFNγ and granzyme-B (**Fig. 6A**). These findings were not limited to $CD8^+$ T cells, as $CD4^+$ T-helper cells were similarly altered in the TME (**Fig. 6B**). These findings provide a preclinical rationale for JAK3i combination immunotherapy and inclusion of anti–PD-1 ICI to further increase antitumor responses.

JAK3i modulates DC-mediated T-cell priming resulting in decreased sensitivity to exhaustion

We previously observed that continuous low-dose JAK3i as monotherapy, or in combination with vaccines, increased T-cell proliferation early after treatment. This suggests that T-cell priming could be modulated by fine-tuning JAK3-activity. To investigate this, we first assessed whether JAK3i directly affected DC-phenotype *in vitro* by treating GM-CSF cultured BMDCs with increasing concentrations of JAK3i during activation with the TLR9-ligand CpG (**Fig. 7A**). We

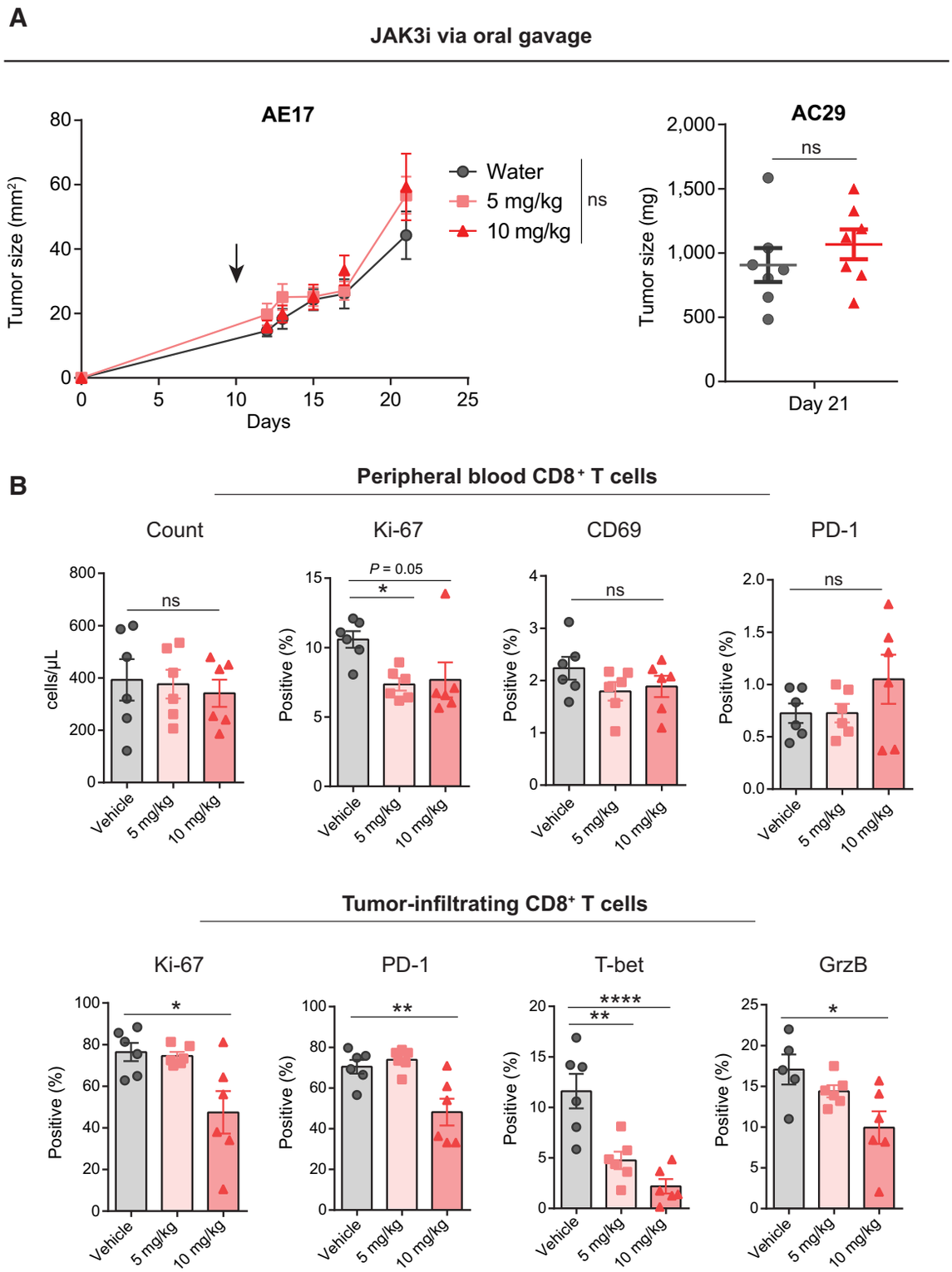

Figure 3.

Twice-daily high-dose JAK3i via oral gavage does not impact tumor growth and inhibits T-cell immunity. **A,** AE17 subcutaneous and AC29 intraperitoneal tumor-bearing mice were treated with the JAK3i PF-06651600 via twice-daily oral gavage starting on day 10, and tumor burden was assessed on day 21. **B,** $CD8^+$ T cells in peripheral blood on day 15 (top) or in the tumor at end stage (bottom) were assessed for proliferation (Ki-67) and activation status using multicolor flow cytometry. Means and SEM are shown with $n = 6$ mice/condition. *, $P < 0.05$; **, $P < 0.01$; ****, $P < 0.0001$. GrzB, granzyme B; ns, nonsignifcant.

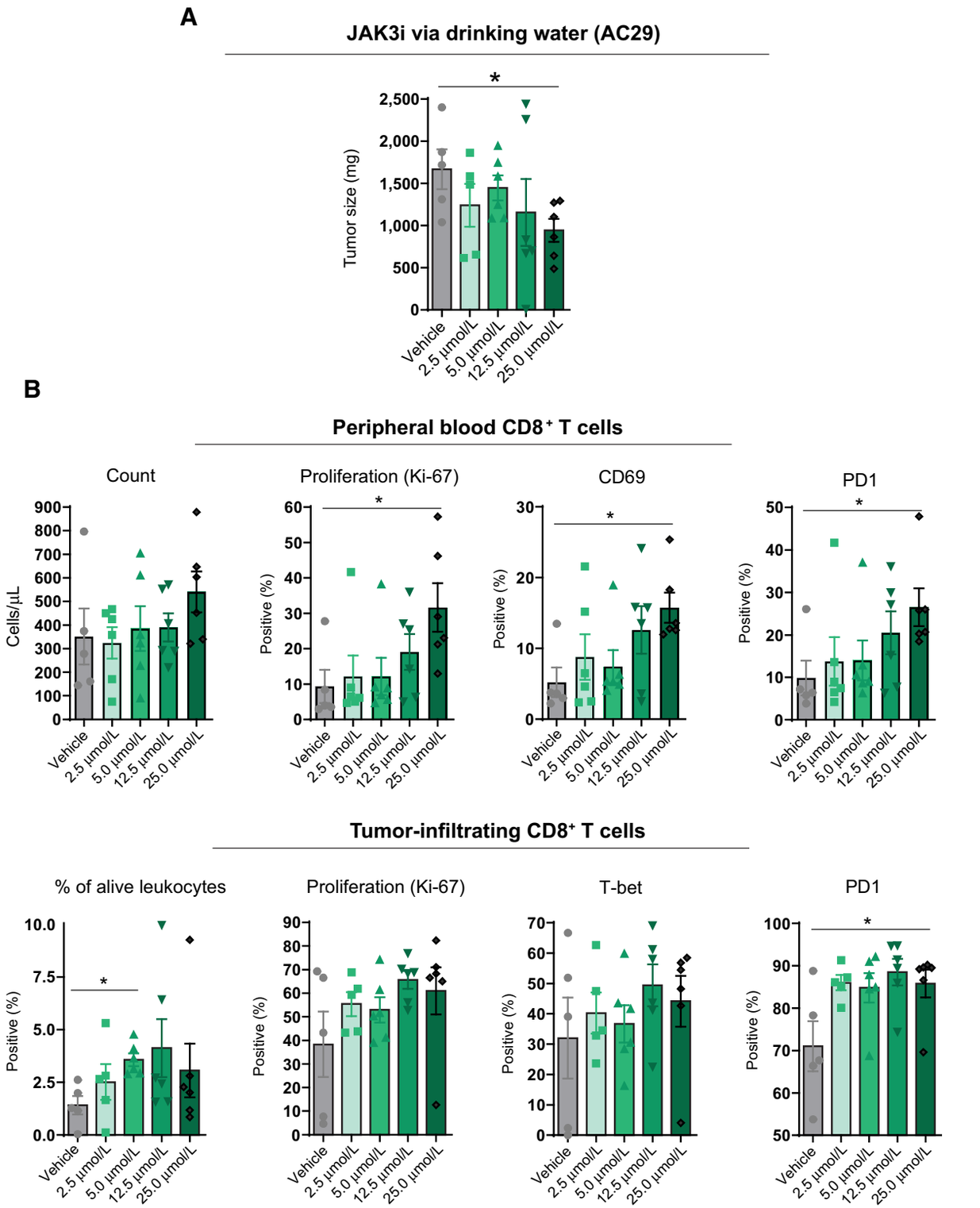

Figure 4.

Continuous low-dose JAK3i at 5.0 mg/kg significantly decreases tumor weight in AC29-bearing mice and improves antitumor T-cell immunity. **A,** AC29 intraperitoneal tumor-bearing mice were treated with the JAK3i PF-06651600 dissolved in drinking water at various prespecified doses, and tumor weight was monitored. **B,** $CD8^+$ T cells in peripheral blood on day 15 (top) or in the tumor at the end of the experiment (day 20; bottom) were assessed for proliferation (Ki67) and activation status using multicolor flow cytometry. Means and SEM are shown with $n = 6$ mice/condition. *, $P < 0.05$.

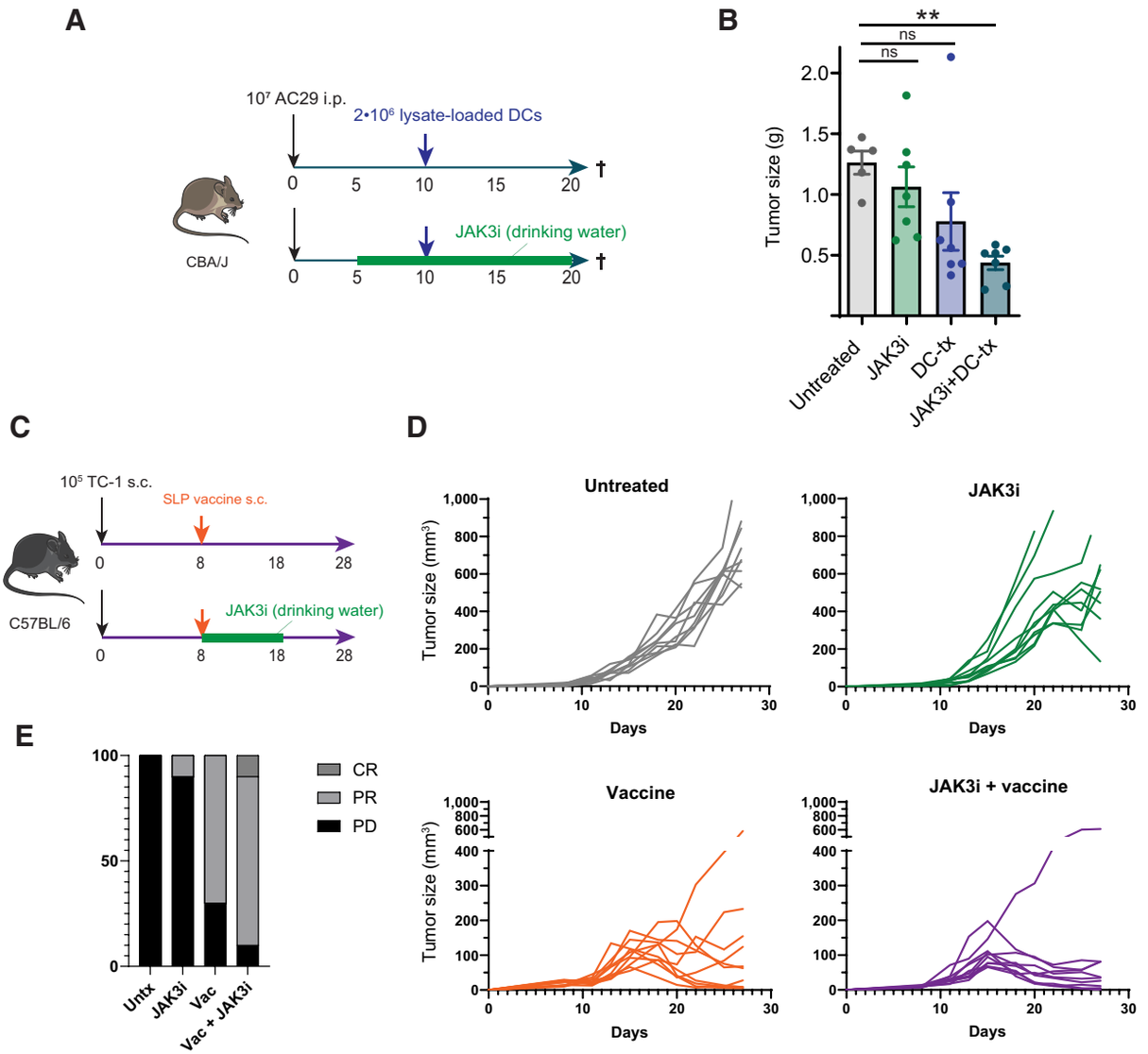

Figure 5.

JAK3i increases cellular and peptide vaccine efficacy. **A** and **B,** Intraperitoneal (i.p.) AC29 and subcutaneous (s.c.) TC-1–bearing mice (**C**) were treated with dendritic cell (DC) therapy or a synthetic-long peptide (SLP) vaccine, respectively, alone or in combination with JAK3i (PF-06651600) at indicated time points. Tumor weight was monitored at end stage in the case of AC29 tumors, and individual tumor size was monitored 3/week in the case of TC-1 (**D**). **E,** Tumor responses were graded as complete response (CR) defined as a complete eradication of tumor (being nonpalpable), partial response (PR) being >30% decrease in tumor volume compared with maximum initial tumor size, and progressive disease less than 30% regression and eventual tumor progression. Means and SEM are shown with $n = 6$–10 mice/condition. Vac, SLP-vaccine; **, $P < 0.01$.

found that DC-viability, co-stimulatory and homing (CCR) receptor expressions were unaltered by JAK3i and MHC class I and II expression was only marginally increased at high concentrations, similar to macrophages (Supplementary Figs. S9, S6–S7). Next, OVA-peptide–loaded DCs were co-cultured with sorted naïve OT-I T cells in the presence or absence of JAK3i and T-cell proliferation and phenotype were assessed. Even at the highest concentration, we found that JAK3i did not impair T-cell expansion or activation capacity (determined by proliferation dye dilution and CD44, PD-1 expression, respectively). However, activated-induced apoptosis and exhaustion (as measured by TOX and CD39 expression) were decreased, suggesting sustainable T-cell activation (**Fig. 7B**). CD25-expression was dose dependently decreased by JAK3i confirming the role of IL2R–JAK3–STAT5 signaling in amplifying CD25 and thus high-affinity IL2R expression (37). Furthermore, 0.1 μmol/L JAK3i-cultured T cells demonstrated increased AE17-OVA killing capacity *in vitro*, albeit not statistically significant, whereas at higher concentrations effector function decreased (**Fig. 7C**). The improved T-cell phenotype observed during priming persisted during the effector phase of the immune response (Supplementary Fig. S9B). These findings indicate that fine-tuning JAK3-activity during priming yields a superior T-cell phenotype that could underlie improved antitumor efficacy *in vivo*.

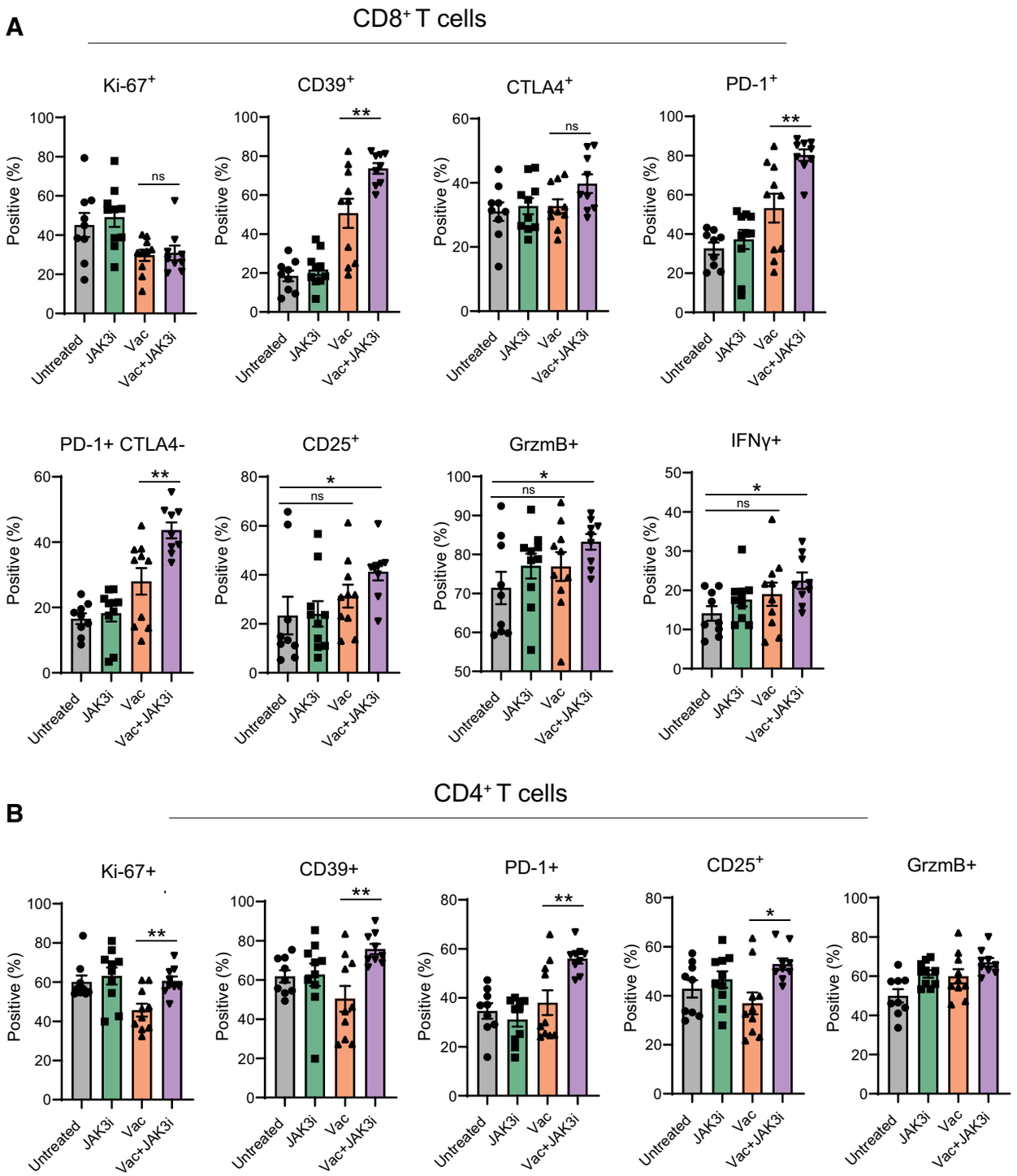

Figure 6.

JAK3i improves peptide vaccine–induced CD8$^+$ and CD4$^+$ T-cell immunity in the tumor microenvironment. CD8$^+$ (**A**) and CD4$^+$ T-helper cell (**B**) proliferation (Ki67) and surface expression of coinhibitory checkpoints or activation markers were assessed in end-stage tumors of the experiment described previously in **Fig. 4C**. Means and SEM are shown with $n = 9$–10 mice/condition. IFNγ, interferon-gamma; *, $P < 0.05$; **, $P < 0.01$.

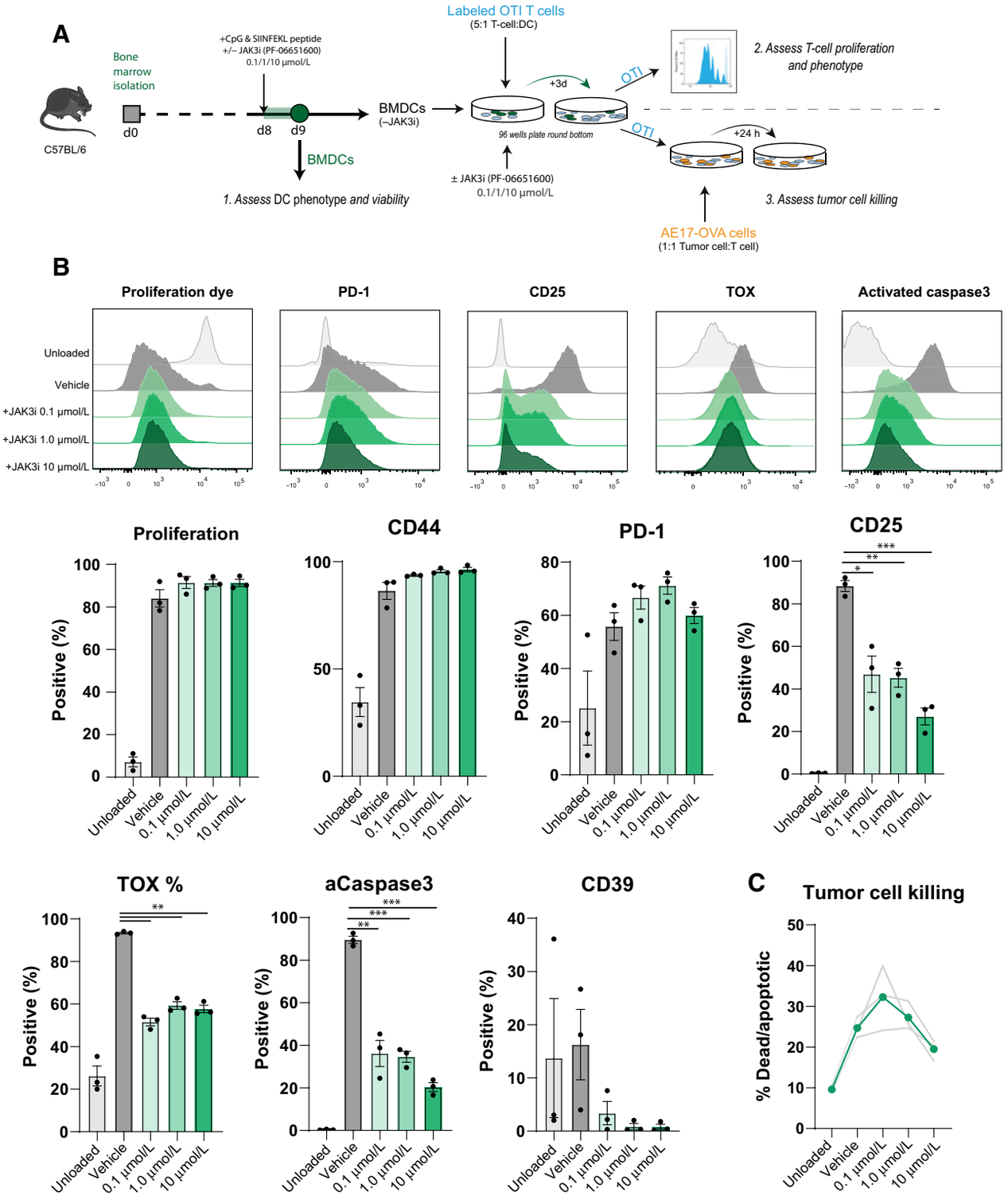

Figure 7.

JAK3i does not impede expansion following DC-mediated priming but rather limits T-cell exhaustion and apoptosis *in vitro*. **A,** Experimental setup of the *in vitro* OT-I T-cell-DC/tumor-cell co-culture system. **B,** Histograms showing T-cell phenotype after 72 hours of co-culture with OVA peptide–loaded DCs in the presence of increasing concentrations of JAK3i ((PF-06651600). **C,** Primed JAK3i-cultured OT-I cells were mixed with AE17-OVA tumor cells for 24 hours, and tumor killing (dead + apoptotic tumor cells) was assessed; *, $P < 0.05$; **, $P < 0.01$; ***, $P < 0.001$.

Discussion

In this study, we found low-dose JAK3i to decrease pSTAT5 expression while preserving T-cell proliferation *in vitro* and to improve T-cell phenotype and tumor load in solid tumor models as monotherapy, and in combination with cellular and peptide-vaccine approaches. JAK3i cancer vaccine combination immunotherapy could be a particularly potent anticancer strategy with cellular and peptide vaccines inducing novel polyfunctional T-cell clones that are preserved and further boosted by JAK3i. This approach differs from current treatments primarily aimed at amplifying existing and often dysfunctional antitumor T-cell responses that are only short-term effective in a proportion of patients with cancer (1, 38). Of note, in a recently described screening assay for T-cell exhaustion reversing compounds, two JAK3i were identified to effectively counter T-cell exhaustion *in vitro* similar to our findings, further solidifying a role for JAK3 in mediating T-cell dysfunction (4). Whether *in vivo* antitumor efficacy of JAK3i is driven solely by effects of JAK3i on T cells or whether other immune cells are involved remains to be further investigated.

With the discovery of more specific JAK3i (e.g., PF-06 and decernotinib) (39), JAK3 can be specifically targeted limiting unwanted action and toxicity as described previously for more broad kinase inhibitors such as Tofacitinib and Ibrutinib (18, 40, 41). Specific, small-molecule inhibitors hold significant advantages compared with antibody-mediated therapies, including route of administration (oral vs. intravenous), lack of antidrug antibody formation and the possibility of timely and graded target inhibition that may be key in case of pleiotropic targets such as the IL2R (42). IL2–IL2R interaction may be essential or deleterious for T-cell effector function and pool size, depending on the strength, duration, and moment of interaction in the antitumor immune response (12, 16). Especially in the setting of vaccination, too early or strong blockade of IL2R signaling following T-cell priming could suppress proper T-cell expansion thereby limiting therapy efficacy. Although we did not assess early T-cell expansion in PB of mice following DC- or SLP-vaccination, the effects of JAK3i monotherapy in PB and the effects on tumor progression indicate that graded JAK3i improves, rather than hampers T-cell activity. Further exploration of JAK3i timing and dosing could further inform about optimal treatment conditions in solid tumor treatment.

Recently, Liu and colleagues (12) demonstrated that chronic IL2-mediated JAK1/3-pSTAT5 signaling in the TME-induced T-cell exhaustion via generation of tryptophan metabolites triggering the aryl hydrocarbon receptor (AhR) in T cells (12). As the authors did not therapeutically target this pathway *in vivo*, our findings with JAK3i complement their findings as JAK3i using PF-06 potently and specifically inhibited STAT5-phosphorylation in T cells and improved T-cell phenotype *in vivo*. Interestingly, Liu and colleagues (12) found that an $IL2^{hi}$ gene signature in multiple solid cancer types but also AML was associated with poor patient survival, indicating that IL2R targeting compounds may act on a wide variety of tumor types, including solid- and non-solid cancer types. Whether our JAK3i acts by limiting pSTAT5-mediated tryptophan metabolism and subsequent AhR-stimulation remains to be investigated.

JAK3 is located downstream of several (common γ-chain) cytokine receptors besides the IL2R that may in part explain our *in vivo* efficacy. Although we found a strong effect of JAK3i on IL4-mediated alternative macrophage polarization *in vitro*, we could not detect this *in vivo* questioning the role of this Th2-related cytokine in the TME. IL4-mediated M2 polarization and T-cell suppression can be induced, however, following radiotherapy limiting its immunogenic effect on $CD8^+$ T cells as documented in a mammary tumor model (43). IL15 and IL7 are two other important cytokines signaling through JAK3-associated receptors whose downstream inhibition could play a role in our tumor models. In contrast with IL2 that is dynamically upregulated following TCR-stimulation by cognate antigen, IL7/IL15 are involved in maintaining survival of naïve and memory T cells during homeostatic conditions (44). Liu and colleagues (12) found IL15 to be unable to exert the same exhausted profile in $CD8^+$ T cells, even though both IL2 and IL15 signal through STAT5. Besides their known effects on $CD8^+$ T cells, common γ-chain cytokines, including IL2 can skew Th-phenotypes, particularly IL2-mediated Th1 induction (44). Although we could not detect changes in IFNγ production by Th-cells following JAK3i *in vivo* modulation through Th-subclass differentiation remains a possibility. The same accounts for Treg that constitutively express high levels of the IL2R and rely on IL2 for their expansion, survival but not for their suppressive function (25, 44, 45). Interestingly, although effector T-cell phenotype was altered by JAK3i, we did not observe changes in Treg frequencies or proliferation at the applied JAK3i dose, possibly due to high intrinsic IL2R expression compensating for decreased downstream signaling in the context of JAK3i (Supplementary Fig. S2B).

We have shown JAK3 to be a novel and effective target for cancer immunotherapy, improving T-cell phenotype and antitumor function depending on the mode of targeting. Our findings lay the groundwork for further efficacy testing in human cancer as monotherapy but more promising in combination with existing immunotherapies.

Authors' Disclosures

J.G. Aerts reports grants and personal fees from BMS, personal fees from MSD and Eli Lilly, grants and personal fees from Amphera, personal fees and other support from BIOCAD, and personal fees from Takeda outside the submitted work; as well as reports a patent for tumor lysate licensed to Amphera and Biomarker for IO licensed to Pamgene. No disclosures were reported by the other authors.

Authors' Contributions

F. Dammeijer: Conceptualization, resources, data curation, software, formal analysis, supervision, validation, investigation, visualization, methodology, writing–original draft, project administration, writing–review and editing. **M. van Gulijk:** Conceptualization, resources, data curation, software, validation, investigation, writing–review and editing. **L. Klaase:** Data curation, investigation, methodology. **M. van Nimwegen:** Data curation, investigation, methodology. **R. Bouzid:** Investigation. **R. Hoogenboom:** Investigation. **M.E. Joosse:** Conceptualization, resources, investigation. **R.W. Hendriks:** Conceptualization, supervision, writing–review and editing. **T. van Hall:** Conceptualization, writing–review and editing. **J.G. Aerts:** Conceptualization, supervision, funding acquisition, project administration, writing–review and editing.

Acknowledgments

The authors report no particular funding sources for this project.

The costs of publication of this article were defrayed in part by the payment of page charges. This article must therefore be hereby marked *advertisement* in accordance with 18 U.S.C. Section 1734 solely to indicate this fact.

Note

Supplementary data for this article are available at Molecular Cancer Therapeutics Online (http://mct.aacrjournals.org/).

Received November 22, 2021; revised April 20, 2022; accepted June 16, 2022; published first June 23, 2022.

References

1. Galon J, Bruni D. Approaches to treat immune hot, altered, and cold tumours with combination immunotherapies. Nat Rev Drug Discov 2019;18:197–218.
2. Waldman AD, Fritz JM, Lenardo MJ. A guide to cancer immunotherapy: from T-cell basic science to clinical practice. Nat Rev Immunol 2020;20:651–68.
3. Dammeijer F, Lau SP, van Eijck CHJ, van der Burg SH, Aerts J. Rationally combining immunotherapies to improve efficacy of immune checkpoint blockade in solid tumors. Cytokine Growth Factor Rev 2017;36:5–15.
4. Marro BS, Zak J, Zavareh RB, Teijaro JR, Lairson LL, Oldstone MBA. Discovery of small molecules for the reversal of T-cell exhaustion. Cell Rep 2019;29:3293–302.
5. McLane LM, Abdel-Hakeem MS, Wherry EJ. CD8 T-cell exhaustion during chronic viral infection and cancer. Annu Rev Immunol 2019;37:457–95.
6. Schietinger A, Philip M, Krisnawan VE, Chiu EY, Delrow JJ, Basom RS, et al. Tumor-specific T-cell dysfunction is a dynamic antigen-driven differentiation program initiated early during tumorigenesis. Immunity 2016;45:389–401.
7. Moore EC, Cash HA, Caruso AM, Uppaluri R, Hodge JW, Van Waes C, et al. Enhanced tumor control with combination mTOR and PD-L1 inhibition in syngeneic oral cavity cancers. Cancer Immunol Res 2016;4:611–20.
8. Eng C, Kim TW, Bendell J, Argilés G, Tebbutt NC, Di Bartolomeo M, et al. Atezolizumab with or without cobimetinib versus regorafenib in previously treated metastatic colorectal cancer (IMblaze370): a multicentre, open-label, phase 3, randomised, controlled trial. Lancet Oncol 2019;20:849–61.
9. Verma V, Jafarzadeh N, Boi S, Kundu S, Jiang Z, Fan Y, et al. MEK inhibition reprograms $CD8^+$ T lymphocytes into memory stem cells with potent antitumor effects. Nat Immunol 2021;22:53–66.
10. Ebert PJR, Cheung J, Yang Y, McNamara E, Hong R, Moskalenko M, et al. MAP kinase inhibition promotes T-cell and antitumor activity in combination with PD-L1 checkpoint blockade. Immunity 2016;44:609–21.
11. Diken M, Kreiter S, Vascotto F, Selmi A, Attig S, Diekmann J, et al. mTOR inhibition improves antitumor effects of vaccination with antigen-encoding RNA. Cancer Immunol Res 2013;1:386–92.
12. Liu Y, Zhou N, Zhou L, Wang J, Zhou Y, Zhang T, et al. IL2 regulates tumor-reactive $CD8^+$ T-cell exhaustion by activating the aryl hydrocarbon receptor. Nat Immunol 2021;22:358–69.
13. Beltra J-C, Bourbonnais S, Bédard N, Charpentier T, Boulangé M, Michaud E, et al. IL2Rβ-dependent signals drive terminal exhaustion and suppress memory development during chronic viral infection. Proc Natl Acad Sci 2016;113:E5444-E53.
14. Kalia V, Sarkar S, Subramaniam S, Haining WN, Smith KA, Ahmed R. Prolonged interleukin-2Ralpha expression on virus-specific $CD8^+$ T cells favors terminal-effector differentiation in vivo. Immunity 2010;32:91–103.
15. Boyman O, Sprent J. The role of interleukin-2 during homeostasis and activation of the immune system. Nat Rev Immunol 2012;12:180–90.
16. Liao W, Lin JX, Leonard WJ. Interleukin-2 at the crossroads of effector responses, tolerance, and immunotherapy. Immunity 2013;38:13–25.
17. O'Shea JJ, Schwartz DM, Villarino AV, Gadina M, McInnes IB, Laurence A. LATJAK-STAT pathway: impact on human disease and therapeutic intervention. Annu Rev Med 2015;66:311–28.
18. Schwartz DM, Kanno Y, Villarino A, Ward M, Gadina M, O'Shea JJ. JAK inhibition as a therapeutic strategy for immune and inflammatory diseases. Nat Rev Drug Discov 2017;16:843–62.
19. Telliez JB, Dowty ME, Wang L, Jussif J, Lin T, Li L, et al. Discovery of a JAK3-selective inhibitor: functional differentiation of JAK3-selective inhibition over pan-JAK or JAK1-selective inhibition. ACS Chem Biol 2016;11:3442–51.
20. Thorarensen A, Dowty ME, Banker ME, Juba B, Jussif J, Lin T, et al. Design of a Janus kinase 3 (JAK3) specific inhibitor 1-((2S,5R)-5-((7H-Pyrrolo[2,3-d]pyrimidin-4-yl)amino)-2-methylpiperidin-1-yl)prop-2-en-1-one (PF-06651600) allowing for the interrogation of JAK3 signaling in humans. J Med Chem 2017;60:1971–93.
21. Dammeijer F, Lievense LA, Kaijen-Lambers ME, van Nimwegen M, Bezemer K, Hegmans JP, et al. Depletion of tumor-associated macrophages with a CSF-1R kinase inhibitor enhances antitumor immunity and survival induced by DC immunotherapy. Cancer Immunol Res 2017;5:535–46.
22. Schulz KR, Danna EA, Krutzik PO, Nolan GP. Single-cell phospho-protein analysis by flow cytometry. Curr Protoc Immunol 2007;8.17:1–20.
23. Herman SEM, Montraveta A, Niemann CU, Mora-Jensen H, Gulrajani M, Krantz F, et al. The bruton tyrosine kinase (BTK) inhibitor acalabrutinib demonstrates potent on-target effects and efficacy in two mouse models of chronic lymphocytic leukemia. Clin Cancer Res 2017;23:2831–41.
24. Pal Singh S, Dammeijer F, Hendriks RW. Role of Bruton's tyrosine kinase in B cells and malignancies. Mol Cancer 2018;17:57.
25. Pandiyan P, Zheng L, Ishihara S, Reed J, Lenardo MJ. $CD4^+CD25^+Foxp3^+$ regulatory T cells induce cytokine deprivation-mediated apoptosis of effector $CD4^+$ T cells. Nat Immunol 2007;8:1353–62.
26. LaPorte SL, Juo ZS, Vaclavikova J, Colf LA, Qi X, Heller NM, et al. Molecular and structural basis of cytokine receptor pleiotropy in the interleukin-4/13 system. Cell 2008;132:259–72.
27. Bosurgi L, Cao YG, Cabeza-Cabrerizo M, Tucci A, Hughes LD, Kong Y, et al. Macrophage function in tissue repair and remodeling requires IL4 or IL13 with apoptotic cells. Science 2017;356:1072–6.
28. Dammeijer F, Lievense LA, Veerman GD, Hoogsteden HC, Hegmans JP, Arends LR, et al. The efficacy of tumor vaccines and cellular immunotherapies in non–small cell lung cancer: a systematic review and meta-analysis. J Clin Oncol 2016;34:3204–12.
29. Hegmans JP, Veltman JD, Lambers ME, de Vries IJ, Figdor CG, Hendriks RW, et al. Consolidative dendritic cell-based immunotherapy elicits cytotoxicity against malignant mesothelioma. Am J Respir Crit Care Med 2010;181:1383–90.
30. Aerts J, de Goeje PL, Cornelissen R, Kaijen-Lambers MEH, Bezemer K, van der Leest CH, et al. Autologous dendritic cells pulsed with allogeneic tumor cell lysate in mesothelioma: from mouse to human. Clin Cancer Res 2018;24:766–76.
31. van Poelgeest MIE, Welters MJP, van Esch EMG, Stynenbosch LFM, Kerpershoek G, van Persijn van Meerten EL, et al. HPV16 synthetic long peptide (HPV16-SLP) vaccination therapy of patients with advanced or recurrent HPV16-induced gynecological carcinoma, a phase II trial. J Transl Med 2013;11:88.
32. Ott PA, Hu Z, Keskin DB, Shukla SA, Sun J, Bozym DJ, et al. An immunogenic personal neoantigen vaccine for patients with melanoma. Nature 2017;547:217–21.
33. Duraiswamy J, Kaluza KM, Freeman GJ, Coukos G. Dual blockade of PD-1 and CTLA-4 combined with tumor vaccine effectively restores T-cell rejection function in tumors. Cancer Res 2013;73:3591–603.
34. Fourcade J, Sun Z, Benallaoua M, Guillaume P, Luescher IF, Sander C, et al. Upregulation of Tim-3 and PD-1 expression is associated with tumor antigen-specific $CD8^+$ T-cell dysfunction in melanoma patients. J Exp Med 2010;207:2175–86.
35. Kortekaas KE, Santegoets SJ, Sturm G, Ehsan I, van Egmond SL, Finotello F, et al. CD39 identifies the $CD4^+$ tumor-specific T-cell population in human cancer. Cancer Immunol Res 2020;8:1311.
36. Duhen T, Duhen R, Montler R, Moses J, Moudgil T, de Miranda NF, et al. Co-expression of CD39 and CD103 identifies tumor-reactive CD8 T cells in human solid tumors. Nat Commun 2018;9:2724.
37. Kim HP, Kelly J, Leonard WJ. The basis for IL2-induced IL2 receptor alpha chain gene regulation: importance of two widely separated IL2 response elements. Immunity 2001;15:159–72.
38. Pai CS, Huang JT, Lu X, Simons DM, Park C, Chang A, et al. Clonal deletion of tumor-specific T cells by interferon-gamma confers therapeutic resistance to combination immune checkpoint blockade. Immunity 2019;50:477–92.
39. Farmer LJ, Ledeboer MW, Hoock T, Arnost MJ, Bethiel RS, Bennani YL, et al. Discovery of VX-509 (decernotinib): a potent and selective janus kinase 3 inhibitor for the treatment of autoimmune diseases. J Med Chem 2015;58:7195–216.
40. Eberl HC, Werner T, Reinhard FB, Lehmann S, Thomson D, Chen P, et al. Chemical proteomics reveals target selectivity of clinical Jak inhibitors in human primary cells. Sci Rep 2019;9:14159.
41. Dunbar A, Joosse ME, de Boer F, Eefting M, Rijnders BJA. Invasive fungal infections in patients treated with Bruton's tyrosine kinase inhibitors. Neth J Med 2020;78:294–6.
42. Oo C, Kalbag SS. Leveraging the attributes of biologics and small molecules, and releasing the bottlenecks: a new wave of revolution in drug development. Expert Rev Clin Pharmacol 2016;9:747–9.
43. Shiao SL, Ruffell B, DeNardo DG, Faddegon BA, Park CC, Coussens LM. TH2-polarized CD4(+) T cells and macrophages limit efficacy of radiotherapy. Cancer Immunol Res 2015;3:518–25.
44. Lin JX, Leonard WJ. The common cytokine receptor γ chain family of cytokines. Cold Spring Harb Perspect Biol 2018;10:a028449.
45. Fontenot JD, Rasmussen JP, Gavin MA, Rudensky AY. A function for interleukin 2 in Foxp3-expressing regulatory T cells. Nat Immunol 2005;6:1142–51.